Supporting Information

Efficient Fluorescent Chemosensor for HSO_4^- Based on a Strategy of Anion-Induced Rotation-Displaced H-Aggregates

Jiajia Chang,[a] Chang Liu,[a] Yan Lu,[a] Song He,[a] Liancheng Zhao[a, b] and Xianshun Zeng[*a]

[a] Key Laboratory of Display Materials & Photoelectric Devices, Ministry of Education, Department of Materials Chemistry, School of Materials Science & Engineering, Tianjin University of Technology, Tianjin 300384, China.

[b] School of Materials Science & Engineering, Harbin Institute of Technology, Harbin 150001, China.

Materials and methods

1. Instruments

All solvents and reagents (analytical grade and spectroscopic grade) were obtained commercially and used as received. NMR spectra were recorded on a Bruker spectrometer at 400 (^{1}H NMR) MHz and 100 (^{13}C NMR) MHz. Chemical shifts (δ values) were reported in ppm down field from internal Me_4Si (^{1}H and ^{13}C NMR). High-resolution mass spectra (HRMS) were acquired on an Agilent 6510 Q-TOF LC/MS instrument (Agilent Technologies, Palo Alto, CA) equipped with an electrospray ionization (ESI) source. Elemental analyses were performed on a Vanio-EL elemental analyzer (Analysensystem GmbH, Germany). UV absorption spectra were recorded on a UV-3600 UV-VIS spectrophotometer (Shimadzu, Japan). Fluorescence measurements were performed using an F-4600 fluorescence spectrophotometer (Hitachi, Japan). Melting points were recorded on a Boethius Block apparatus and are uncorrected.

2. Synthesis of L1-L4

2.1 Synthesis of L1

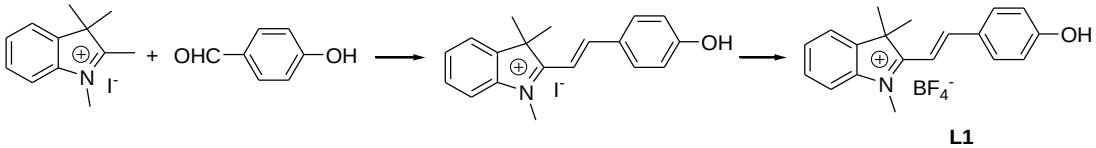

L1

To a 50 ml flask, was charged N-methyl-2,3,3'-trimethylindolium iodide (602 mg, 2.0 mmol), 4-hyrdoxybenzoaldehyde (244 mg, 2 mmol) and anhydrous ethanol (15 mL). The reaction mixture was washed with nitrogen flow for 30 min to remove oxygen, and then stirred at 80 ^{o}C for 72 h in dark. After cooling to room temperature, the solvent was removed under reduced pressure. The residue was dissolved

in DMF (10 mL) and $NaBF_4$ (1.10 g, 10.0 mmol) was added in one portion to the solution. The suspension was stirred for another 3 h in dark at room temperature. The suspension was filtered through a short celite column and the filtrate was condensed to dryness under reduced pressure. The residue was recrystallized from acetonitrile (10 mL) and dichloromethane (10 mL). **L1** was obtained as a brownish powder (0.606 g) in 83% yield; mp: 113 ^{o}C-116 ^{o}C; HRMS (ESI-TOF) m/z: $[M - BF_4^-]^+$ Calcd for $C_{19}H_{20}NO$ 278.1545; Found 278.1546; ^{1}H NMR (400 MHz, DMSO-d_6) (δ, ppm) 8.35 (d, 1H, J = 16.4 Hz, ethenyl), 8.12 (d, 2H, J = 8.8 Hz, phenyl), 7.83 (d, 2H, J = 7.2 Hz, indolinyl), 7.61(t, 1H, J = 7.2 Hz, indolinyl), 7.57 (t, 1H, J = 7.2 Hz, indolinyl), 7.45(d, 1H, J = 16.4 Hz, ethenyl), 6.95 (d, 2H, J = 8.8 Hz, phenyl), 4.07 (s, 3H, N-Me), 1.76 (s, 6H, Me); ^{13}C NMR (100 MHz, DMSO-d_6) (δ, ppm) 182.37, 163.93, 154.61, 144.13, 142.78, 134.58, 129.82, 129.73, 129.99, 123.75, 117.29, 115.66, 110.35, 52.71, 35.22, 26.66; Calcd for $C_{19}H_{20}BF_4NO{\cdot}0.5CH_2Cl_2$: C 57.45, H 5.19, N 3.44; Found: C 57.15, H 5.42, N, 3.37.

2.2 Synthesis of L2

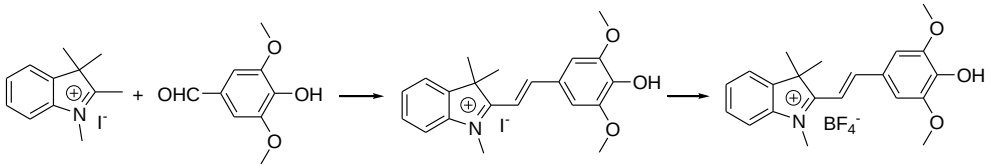

L2

The reaction was performed with 3,5-dimethoxyl-4-hydroxybenzoaldehyde (0.364 g, 2.0 mmol) and N-methyl-2,3,3'-trimethylindolium iodide (0.602 g, 2.0 mmol) by using the same method as that for **L1**. A yellow solid was obtained (0.655 g): Yield 77%; mp 222-224 ^{o}C; HRMS (ESI-TOF) m/z: $[M - BF_4^-]^+$ Calcd for $C_{21}H_{24}NO_3$ 338.1756; Found 338.1760; ^{1}H NMR (400 MHz, DMSO-d_6) (δ, ppm) 8.39 (d, 1H, J = 16.0 Hz, ethenyl), 7.89 (d, 1H, J = 8.4 Hz, indolinyl), 7.86 (d, 1H, J = 8.4 Hz, indolinyl), 7.68-7.60 (m, 4H, indolinyl, aryl), 7.50 (d, 1H, J = 16.0 Hz, ethenyl), 4.16 (s, 3H, N-Me), 3.95 (s, 6H, OMe), 1.83 (s, 6H, Me); ^{13}C NMR (100 MHz, DMSO-d_6) (δ, ppm) 181.70, 155.04, 149.24, 144.05, 142.81, 129.72, 129.46, 125.95, 123.64, 115.38, 110.20, 110.07, 57.42, 52.53, 34.97, 26.66; Calcd for $C_{21}H_{24}BF_4NO_3$: C, 59.32; H, 5.69; N, 3.29; Found: C 59.18, H 5.58, N, 3.19.

2.3 Synthesis of L3

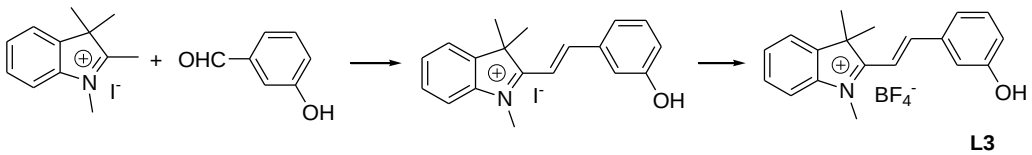

L3

The reaction was performed with 3-hydroxybenzoaldehyde (0.244 g, 2.0 mmol) and

N-methyl-2,3,3'-trimethylindolium iodide (0.602 g, 2.0 mmol) by using the same method as that for **L1**. A yellow solid was obtained (0.621 g): Yield 85%; 216-218 ^{o}C; HRMS (ESI-TOF) m/z: $[M - BF_4^-]^+$ Calcd for $C_{19}H_{20}NO$ 278.1545; Found 278.1545; Calcd: 278.1539; ^{1}H NMR (400 MHz, DMSO-d_6) (δ, ppm) 8.33 (d, 1H, J = 16.4 Hz, ethenyl), 7.93-7.87 (m, 2H, indolinyl, phenyl), 7.65-7.41 (m, 5H, indolinyl, phenyl, ethenyl), 7.39 (t, 1H, J = 8.0 Hz, phenyl), 7.05 (dd, 1H, J = 8.0 Hz; 2.0 Hz, phenyl), 4.16 (s, 3H, N-Me), 1.78 (s, 6H, Me); ^{13}C NMR (100 MHz, DMSO-d_6) (δ, ppm) 182.92, 158.72, 154.08, 144.56, 142.76, 136.78, 131.20, 130.47, 129.96, 123.85, 122.59, 121.29, 117.34, 116.26, 114.18, 53.25, 35.60, 26.22; Calcd for $C_{19}H_{20}BF_4NO$: C 62.49, H 5.52, N 3.84; Found: C 62.45, H 5.46, N, 3.66.

2.4 Synthesis of L4

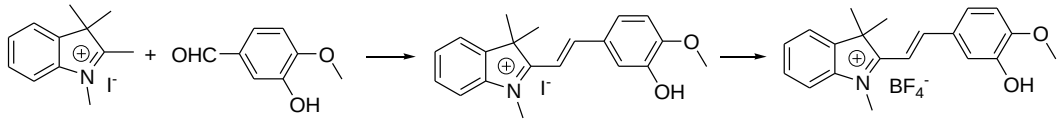

L4

The reaction was performed with 4-methoxyl-3-hydroxybenzoaldehyde (0.304 g, 2.0 mmol) and N-methyl-2,3,3'-trimethylindolium iodide (0.602 g, 2.0 mmol) by using the same method as that for **L1**. A yellow solid was obtained (0.656 g): Yield 83%; mp 216-218 ^{o}C; HRMS (ESI-TOF) m/z: $[M - BF_4^-]^+$ Calcd for $C_{20}H_{22}NO_2$ 308.1651; Found 308.1650; ^{1}H NMR (400 MHz, DMSO-d_6) (δ, ppm) 9.39 (s, 1H, OH), 8.30 (d, 1H, J = 16.4 Hz, ethenyl), 7.86-7.81 (m, 2H, phenyl, indolinyl), 7.71 (dd, 1H, J = 8.4 Hz, 2.0 Hz, indolinyl), 7.66(d, 1H, J = 2.0 Hz, phenyl), 7.62-7.55 (m, 2H, indolinyl), 7.43(d, 1H, J = 16.4 Hz, ethenyl), 7.14 (d, 1H, J = 8.4 Hz, phenyl), 4.09 (s, 3H, N-Me), 3.92 (s, 3H, OMe), 1.76 (s, 6H, Me); ^{13}C NMR (100 MHz, DMSO-d_6) (δ, ppm) 182.34, 154.56, 154.01, 147.84, 144.18, 142.74, 129.78, 128.65, 126.65, 123.72, 116.63, 115.70, 112.93, 111.23, 57.00, 52.74, 35.14, 26.50; Calcd for $C_{20}H_{22}BF_4NO_2$: C, 60.78; H, 5.61; N, 3.54; Found: C 60.81, H 5.37, N, 3.32.

3. Solutions for Spectroscopy.

The fluorescence and absorption titrations were carried out in ethanol-water (1:1, v/v). The dyes **L1-L4** and anions were dissolved in ethanol-deionized (v/v, 1 : 1) to obtain 10^{-3} M stock solutions. Before spectroscopic measurements, the solution was freshly prepared by diluting the high concentration stock solution to the corresponding solution. All of the experiments were performed at barometric pressure and room temperature.

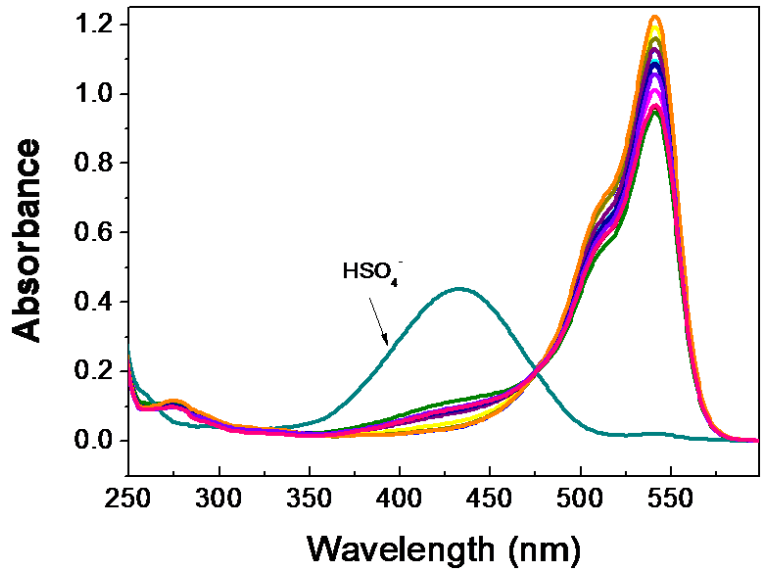

Fig. S1 UV-vis responses of the chemosensor **L1** (10 μM) upon the addition of the sodium salts (10.0 equiv) of PO_4^{3-}, HPO_4^{2-}, $H_2PO_4^-$, NO_3^-, SO_4^{2-}, HSO_4^-, Cl^-, CO_3^{2-}, F^-, and Ac^- in H_2O-EtOH (1:1,v/v).

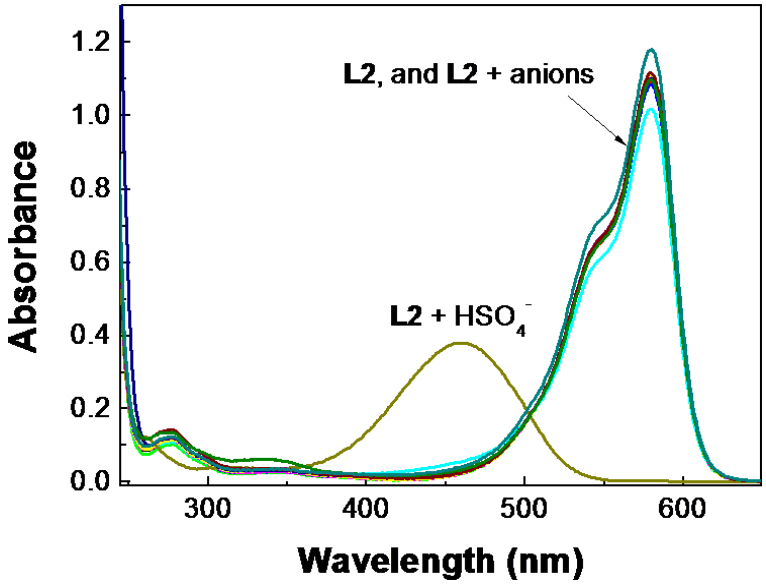

Fig. S2 UV-vis responses of the chemosensor **L2** (10 μM) upon the addition of the sodium salts (10.0 equiv) of PO_4^{3-}, HPO_4^{2-}, $H_2PO_4^-$, NO_3^-, SO_4^{2-}, HSO_4^-, Cl^-, CO_3^{2-}, F^-, and Ac^- in H_2O-EtOH (1:1,v/v).

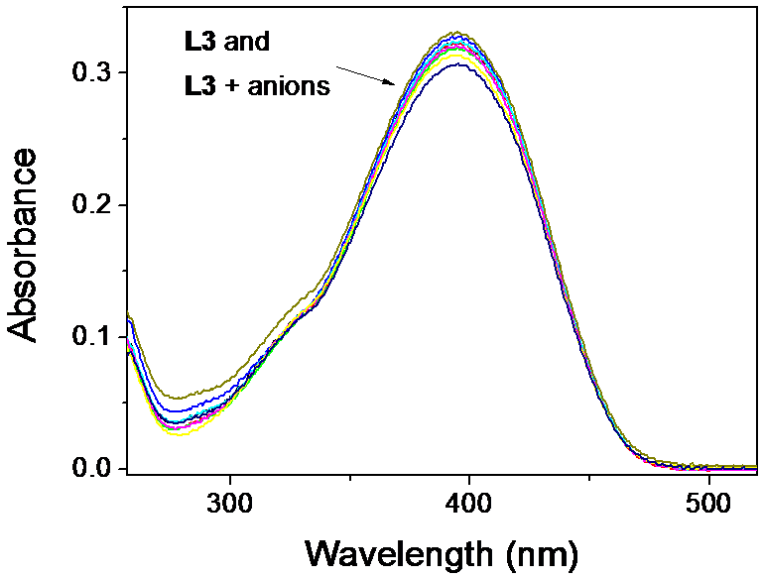

Fig. S3 UV-vis responses of **L3** (10 μM) upon the addition of the sodium salts (10.0 equiv) of PO_4^{3-}, HPO_4^{2-}, $H_2PO_4^-$, NO_3^-, SO_4^{2-}, HSO_4^-, Cl^-, CO_3^{2-}, F^-, and Ac^- in H_2O-EtOH (1:1,v/v).

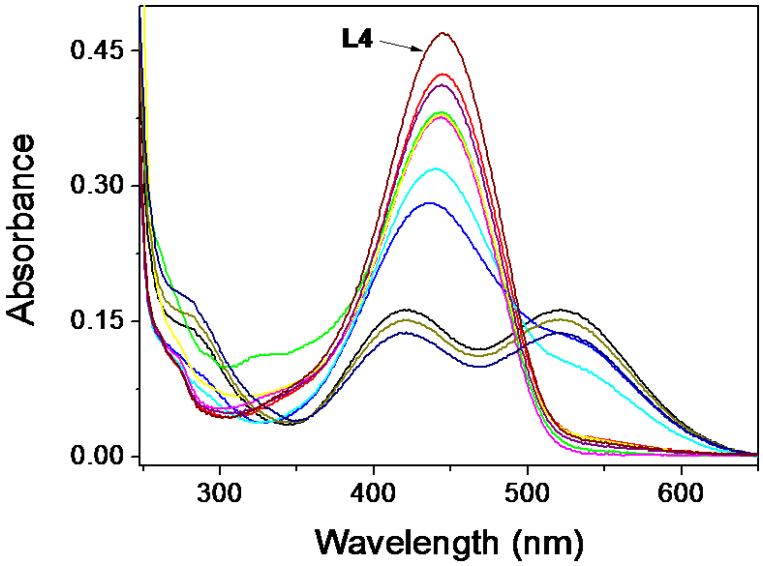

Fig. S4 UV-vis responses of **L4** (10 μM) upon the addition of the sodium salts (10.0 equiv) of PO_4^{3-}, HPO_4^{2-}, $H_2PO_4^-$, NO_3^-, SO_4^{2-}, HSO_4^-, Cl^-, CO_3^{2-}, F^-, and Ac^- in H_2O-EtOH (1:1,v/v).

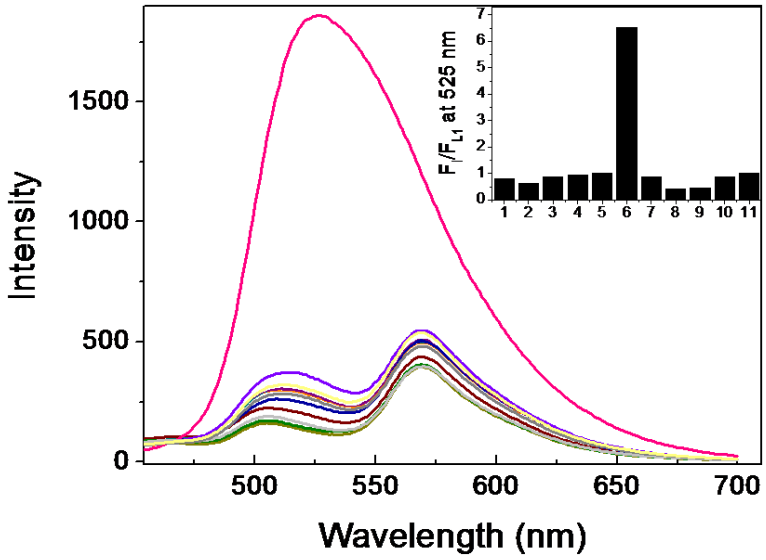

Figure S5. Fluorescence spectra of **L1** (10.0 μM) upon the addition of the sodium salts (10.0 equiv.) of various anion in ethanol/H_2O (1 : 1, v/v). Inset: histogram representing the fluorescence changes of **L1** at 525 nm in the presence of anions. From 1 to 11: PO_4^{3-}, HPO_4^{2-}, $H_2PO_4^-$, NO_3^-, SO_4^{2-}, HSO_4^-, Cl^-, CO_3^{2-}, F^-, Ac^-, and **L1** alone. For the entire test, excitation and emission were performed at 434 and 525 nm.

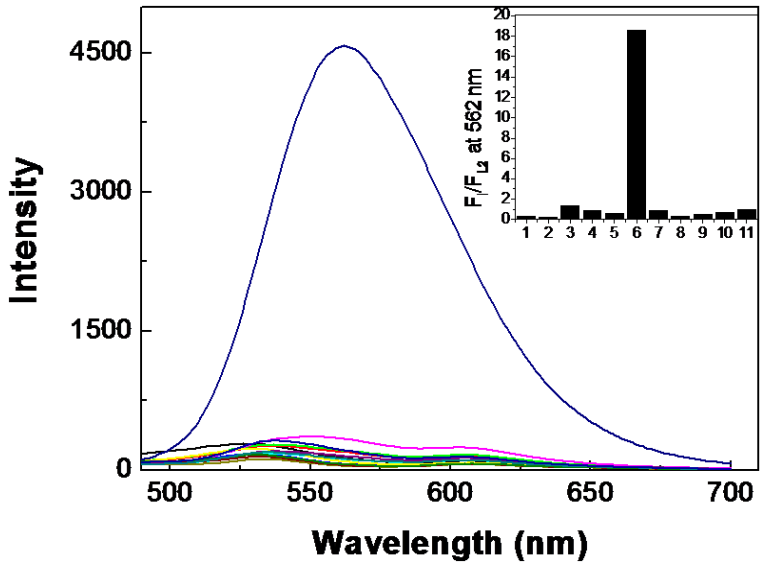

Figure S6. Fluorescence spectra of **L2** (10.0 μM) upon the addition of the sodium salts (10.0 equiv.) of various anion in ethanol/H_2O (1 : 1, v/v). Inset: histogram representing the fluorescence changes of **L2** at 552 nm in the presence of anions. From 1 to 11: PO_4^{3-}, HPO_4^{2-}, $H_2PO_4^-$, NO_3^-, SO_4^{2-}, HSO_4^-, Cl^-, CO_3^{2-}, F^-, Ac^-, and **L2** alone. For the entire test, excitation and emission were performed at 458 and 562 nm.

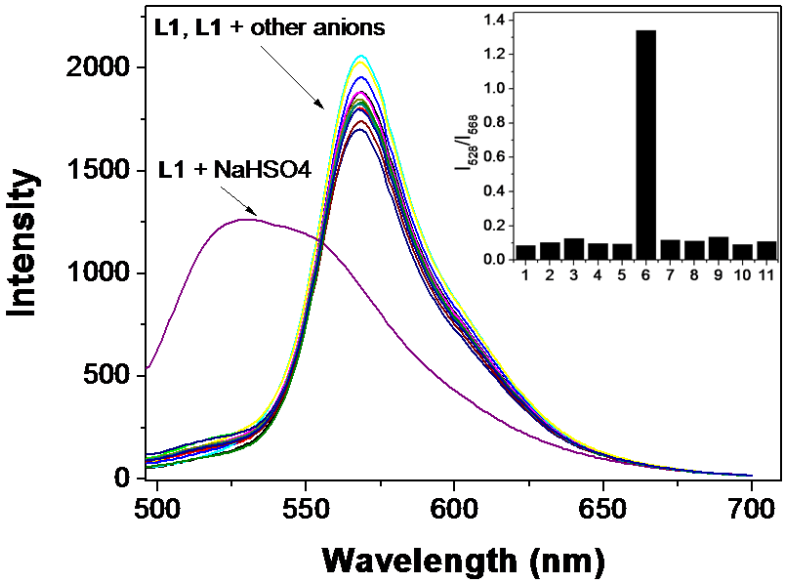

Figure S7. Fluorescence spectra of **L1** (10.0 μM) upon the addition of sodium salts (10.0 equiv.) of various anion in ethanol/H_2O (1 : 1, v/v). Inset: Histogram representing the ratio changes of fluorescence intensities at 528 nm and 568 nm of **L1** (10 μM) in H_2O-EtOH (1: 1, v/v) in the presence of 10.0 equiv. of anions and **L1** alone. 1: **L1** + PO_4^{3-}, 2: **L1** + HPO_4^{2-}, 3: **L1** + $H_2PO_4^-$, 4: **L1** + NO_3^-, 5: **L1** + SO_4^{2-}, 6: **L1** + HSO_4^-,7: **L1** + Cl^-, 8: **L1** + CO_3^{2-}, 9: **L1** + F^-, 10: **L1** + Ac^- and 11: **L1** alone. λ_{ex} = 476 nm.

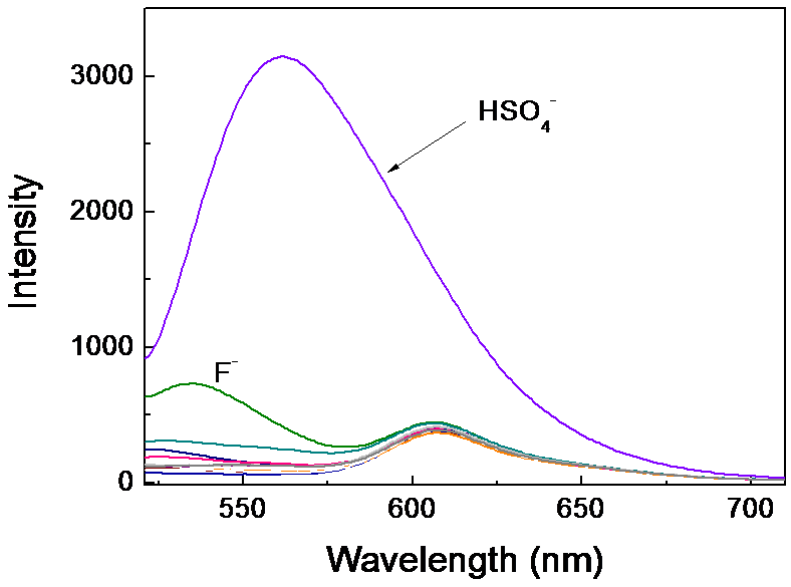

Figure S8. Fluorescence spectra of **L2** (10.0 μM) upon the addition of the sodium salts (10.0 equiv.) of PO_4^{3-}, HPO_4^{2-}, $H_2PO_4^-$, NO_3^-, SO_4^{2-}, HSO_4^-, Cl^-, CO_3^{2-}, F^-, and Ac^- in ethanol/H_2O (1 : 1, v/v). For the entire test, excitation was performed at 501 nm.

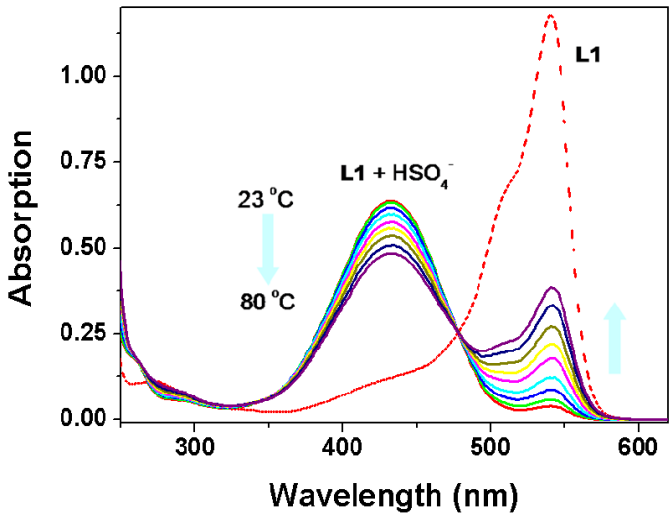

Figure S9. Absorption spectra for **L1** (10.0 μM) in the presence of 10 equiv. of HSO_4^- in EtOH-H_2O (1 : 1, v/v) at different temperatures: 23, 33, 43, 53, 63, 68, 73, 78, 80 °C. The red dash line represents the free **L1**.

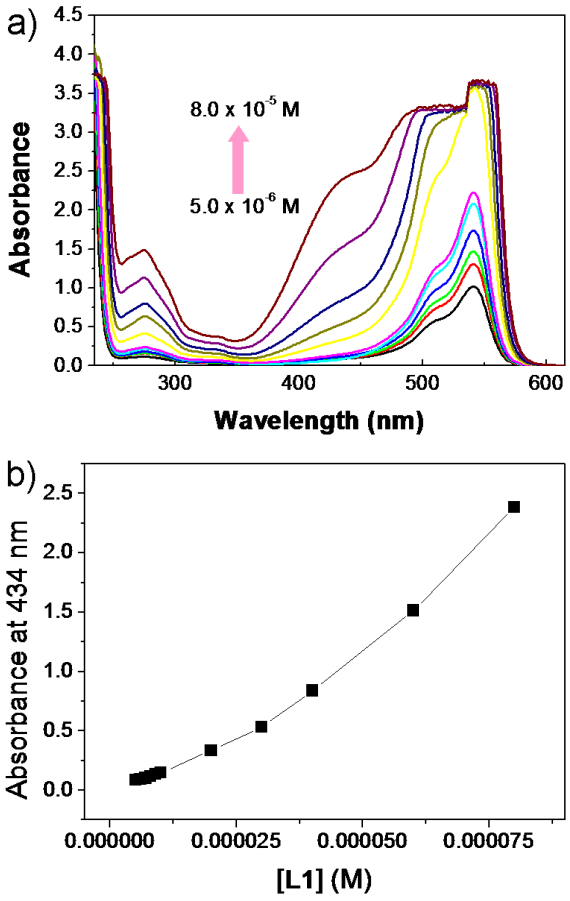

Figure S10. Concentration-dependent UV/Vis absorption spectra. a) concentration-dependent UV/Vis absorption spectra of **L1** in ethanol/H_2O (1 : 1, v/v) from 5.0×10^{-6} M to 8.0×10^{-5} M; b) the concentration-dependent relationship of **L1** at 434 nm.

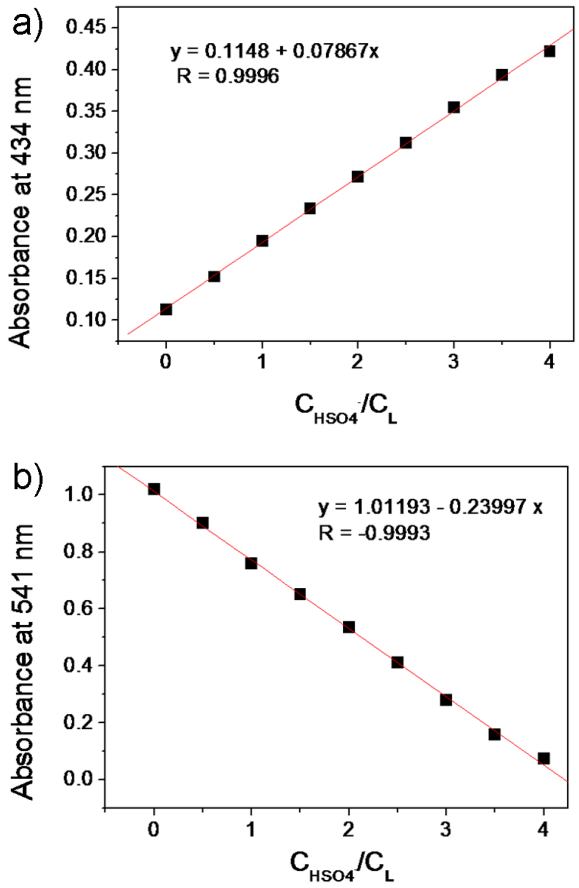

Figure S11. The linear changes of the absorbances of **L1** at 434 nm (a) and at 541 nm (b) as a function of HSO_4^- concentration. For both a) and b), $[HSO_4^-]/[\mathbf{L1}]$: 0, 0.5, 1.0, 1.5, 2.0, 2.5, 3.0, 3.5, 4.0 equivalents.

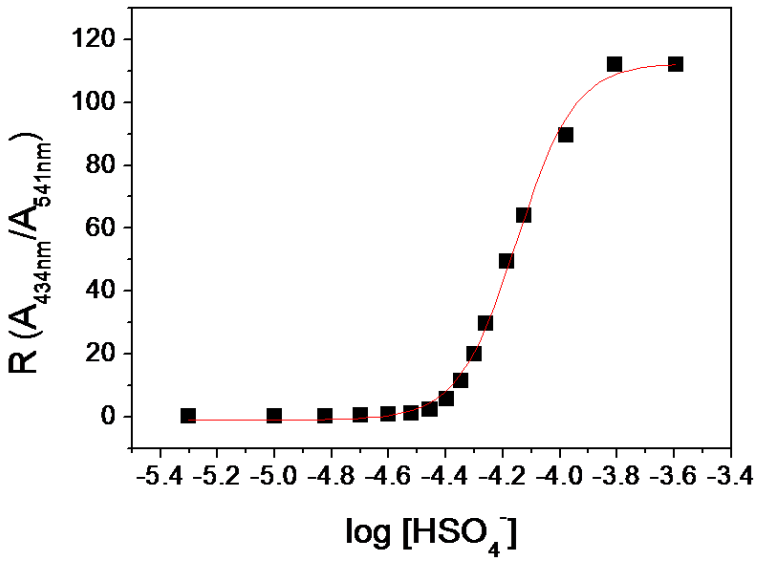

Figure S12. Curve of absorbance intensity ratio (A_{434}/A_{541}) of **L1** versus increasing concentration of HSO_4^-. The concentration of **L1** was 10 μM. The dissociation constant K_d was deduced to be 7.04×10^{-5} M (with correlation coefficient R = 0.997)**.**

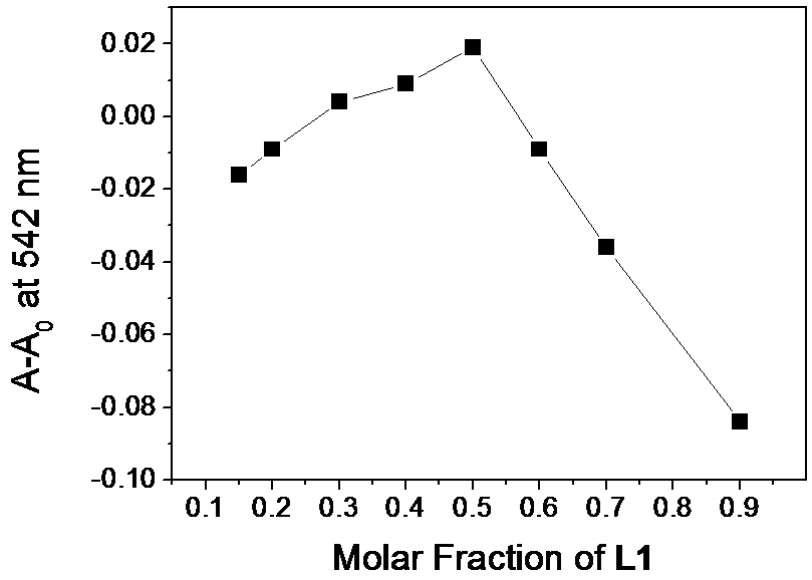

Figure S13. Job's plot of **L1** in ethanol/H_2O (1:1, v/v) showing the 1:1 stoichiometry of the complex between HSO_4^- anion and **L1**. The total concentration of [**L1**] and [HSO_4^-] is 10^{-5} mol/L. Absorbance is recorded at 542 nm.

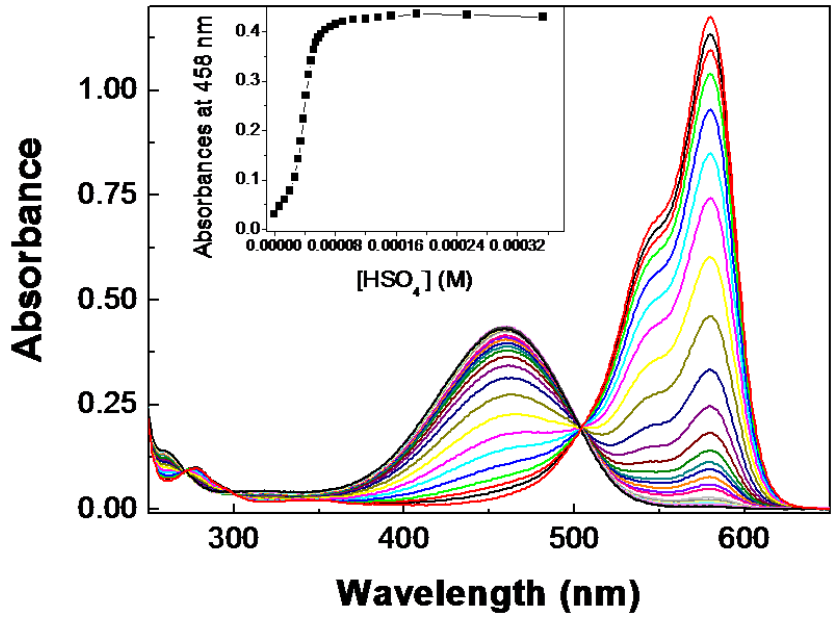

Figure S14. Absorption spectra of the chemosensor **L2** (10.0 μM) to increasing concentrations of HSO_4^- in H_2O-EtOH (1: 1, v/v). [HSO_4^-]/[**L2**] = 0, 0.63, 1.26, 1.89, 2.52, 3.15, 3.77, 4.40, 5.03, 5.66, 6.29, 6.92, 8.18, 9.44, 13.21, 19.50, 32.08. Inset: the absorbances of **L2** at 458 nm as a function of the HSO_4^- concentrations.

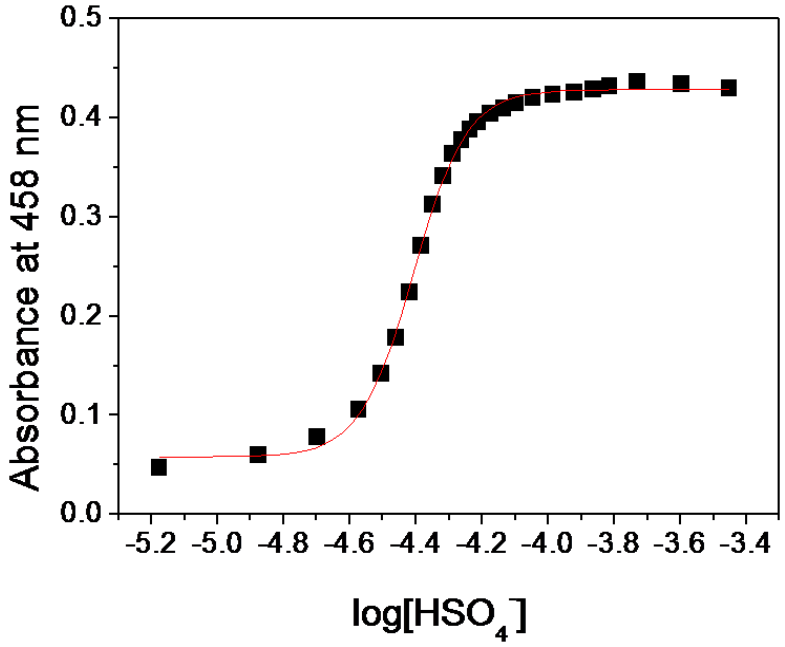

Figure S15. Curve of absorbances of **L2** versus increasing concentration of HSO_4^-. The concentration of **L2** was 10 μM. The dissociation constant K_d was deduced to be 3.91×10^{-5} M (with correlation coefficient $R = 0.998$)**.**

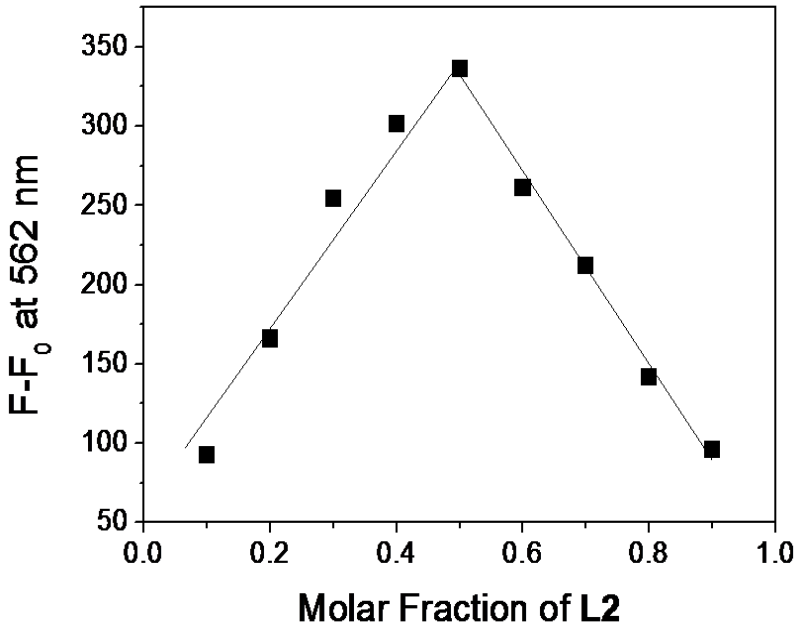

Figure S16. Job's plot of **L2** in ethanol/H_2O (1:1, v/v) showing the 1:1 stoichiometry of the complex between HSO_4^- and **L2**. The total concentration of [**L2**] and [HSO_4^-] is 10^{-5} mol/L. Fluorescence intensity is recorded at 562 nm.

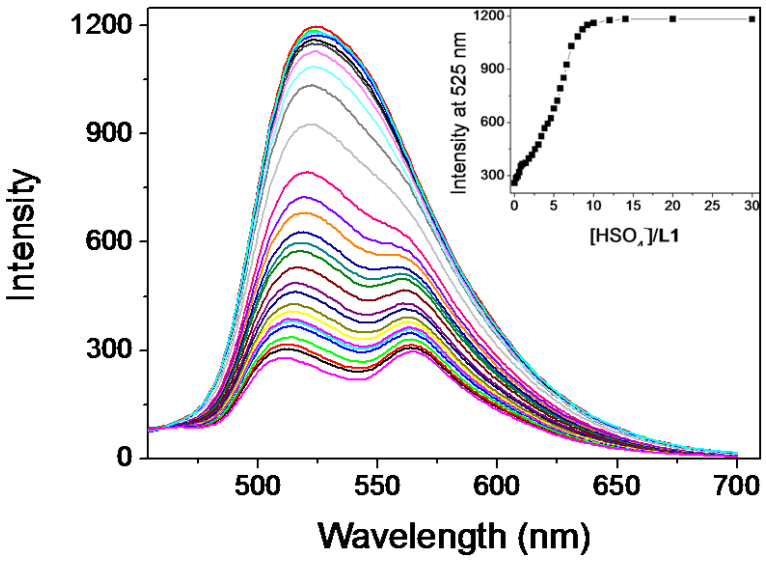

Figure 17. Fluorescent titration spectra of **L1** (6.0 μM) in the presence of different concentrations of HSO_4^- in ethanol-water (1 : 1, v/v), [HSO_4^-]/[**L1**] = 0, 0.2, 0.4, 0.6, 0.8, 1.0, 1.4, 1.8, 2.2, 2.6, 3.0, 3.4, 3.8, 4.2, 4.6, 5.0, 5.4, 5.8, 6.2, 6.6, 7.0, 8.0, 8.6, 9.2, 10.0, 12.0, 14.0, 20.0, 30.0. Inset: the fluorescence intensities of **L1** at 525 nm as a function of the HSO_4^- concentrations. λ_{ex} = 434 nm.

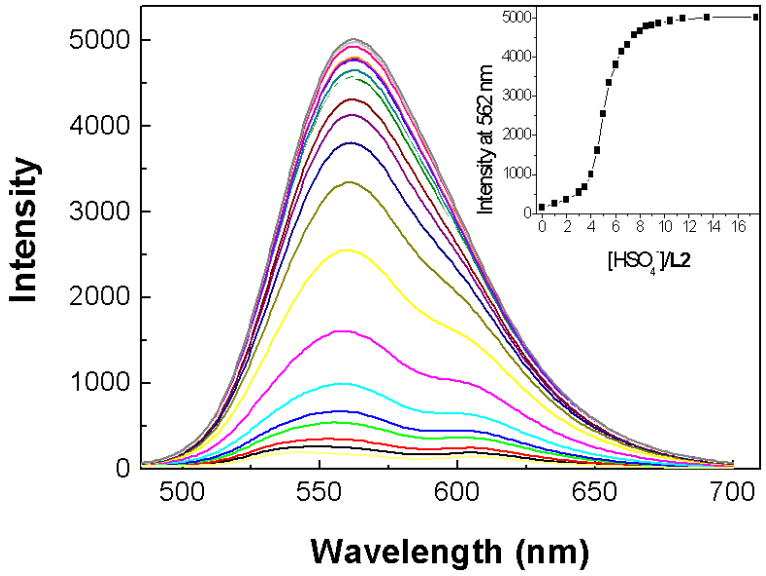

Figure 18. Fluorescent titration spectra of **L2** (6.0 μM) in the presence of different concentrations of HSO_4^- in ethanol-water (1 : 1, v/v), [HSO_4^-]/[**L2**] = 0, 1.0, 2.0, 3.0, 3.5, 4.0, 4.5, 5.0, 5.5, 6.0, 6.5, 7.0, 7.5, 8.0, 8.5, 9.0, 9.5, 10.5, 11.5, 13.5, 17.5. Inset: the fluorescence intensities of **L2** at 562 nm as a function of the HSO_4^- concentrations. λ_{ex} = 458 nm.

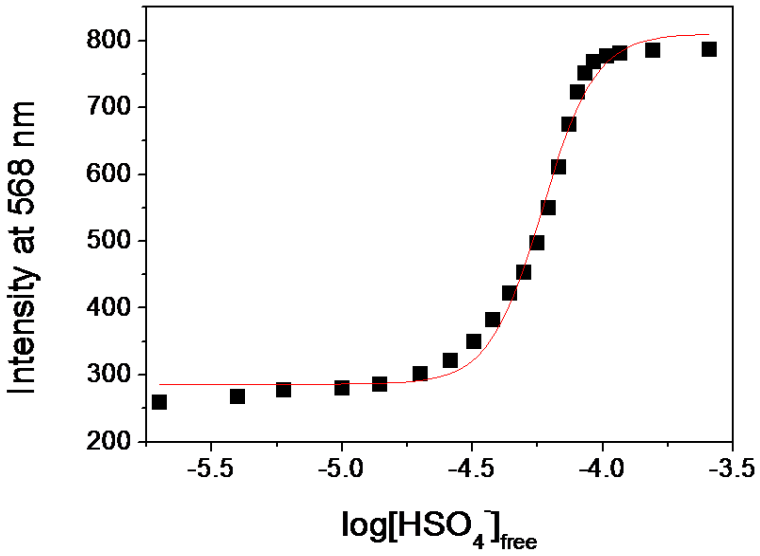

Figure S19. Curve of fluorescence intensity of **L1** (6 μM) at 568 nm versus increasing concentration of HSO_4^-. The dissociation constant K_d was deduced to be 5.86 × 10^{-5} M (with correlation coefficient R = 0.9913)**.**

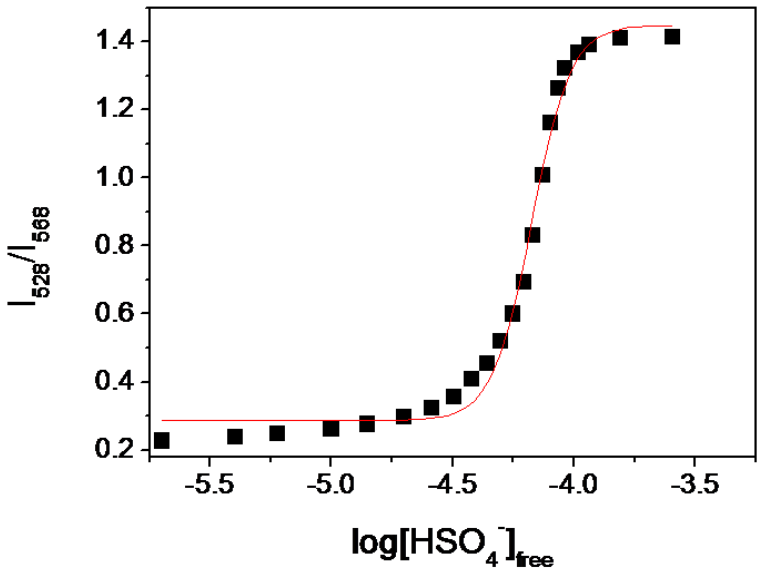

Figure S20. Curve of fluorescence intensity ratio (F_{528}/F_{568}) of **L1** (6 μM) versus increasing concentration of HSO_4^-. The dissociation constant K_d was deduced to be 6.68× 10^{-5} M (with correlation coefficient R = 0.9921)**.**

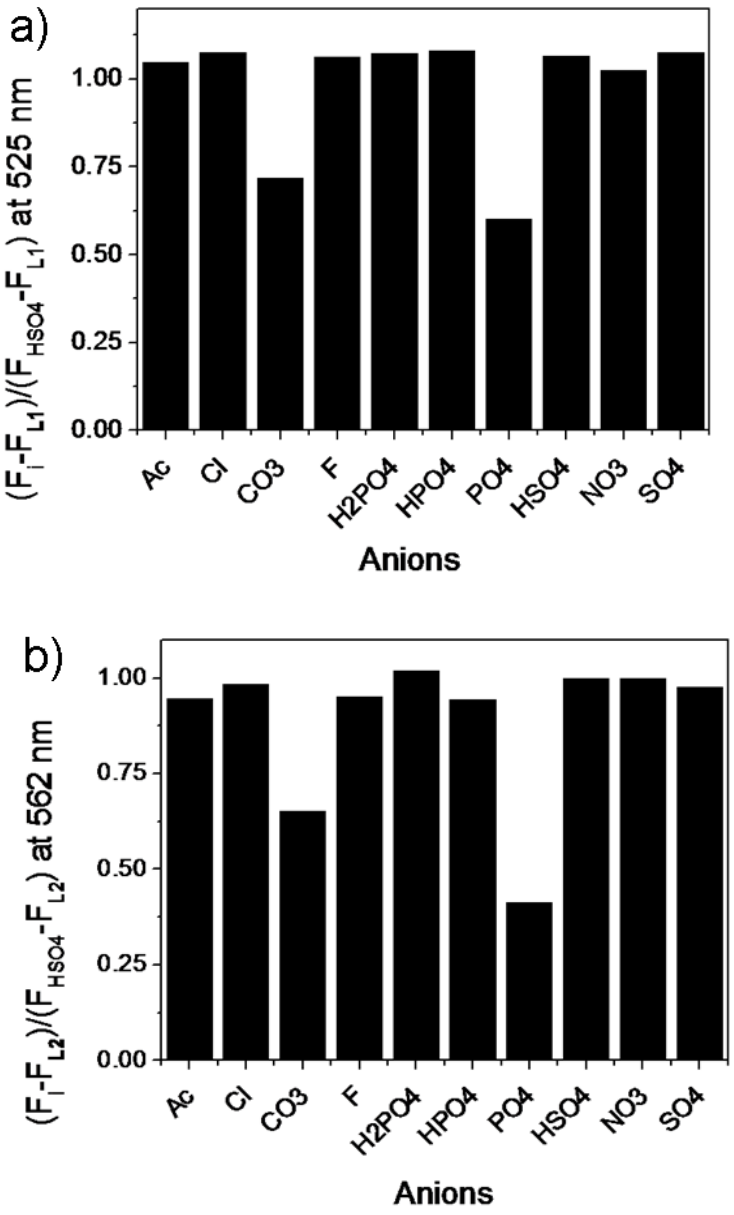

Figure S21. a) Change in the ratio ((F_i - $F_{\mathbf{L1}}$)/(F_{HSO4} - $F_{\mathbf{L1}}$)) of fluorescence intensity of **L1** at 525 nm upon the addition of 10 equiv. of HSO_4^- in the presence of 5 equiv. of back anions in ethanol-water (1 : 1, v/v). λ_{ex} = 434 nm. Slit: 10.0 nm. b) Change in the ratio ((F_i - $F_{\mathbf{L2}}$)/(F_{HSO4} - $F_{\mathbf{L2}}$)) of fluorescence intensity of **L2** at 562 nm upon the addition of 10 equiv. of HSO_4^- in the presence of 5 equiv. of back anions in ethanol-water (1 : 1, v/v). λ_{ex} = 458 nm. Slit: 10.0 nm.

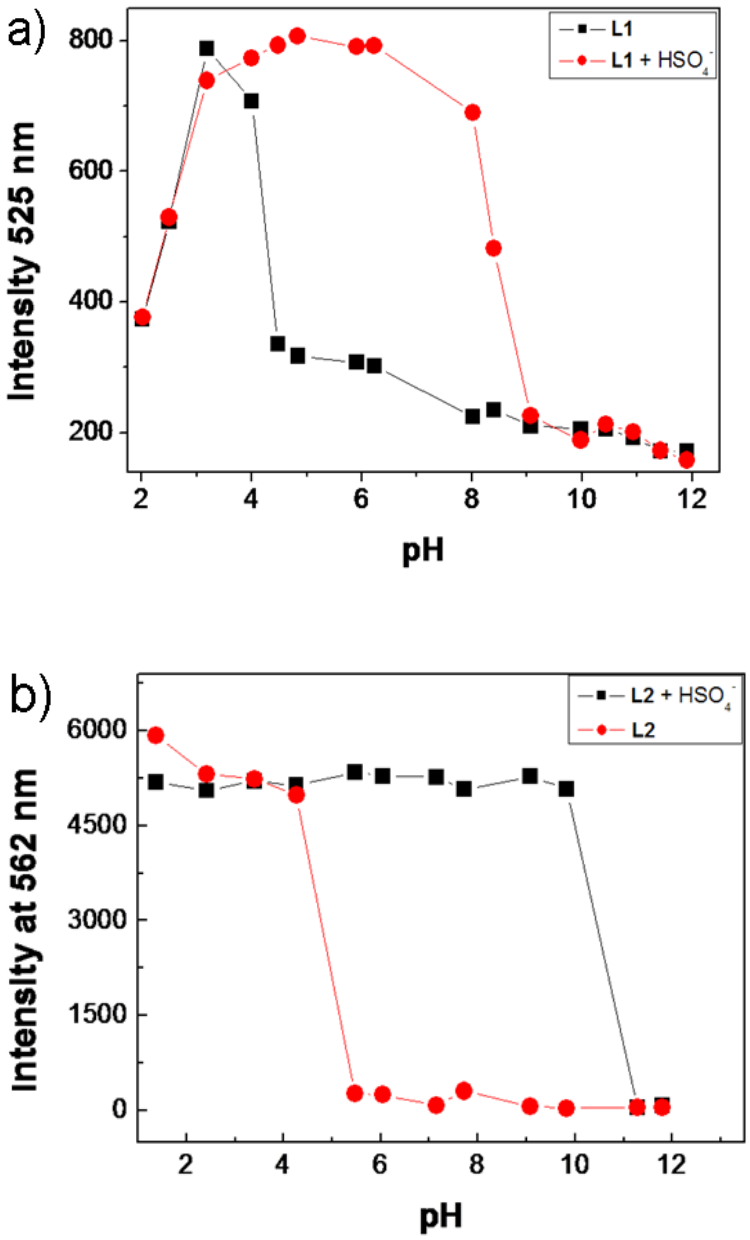

Figure S22. pH profile. a) Profile of pH dependence of the fluorescence intensity of **L1** at 525 nm in the absence and presence of HSO_4^- in ethanol-water (1 : 1, v/v). b) Profile of pH dependence of the fluorescence intensity of **L2** at 562 nm in the absence and presence of HSO_4^- in ethanol-water (1 : 1, v/v).

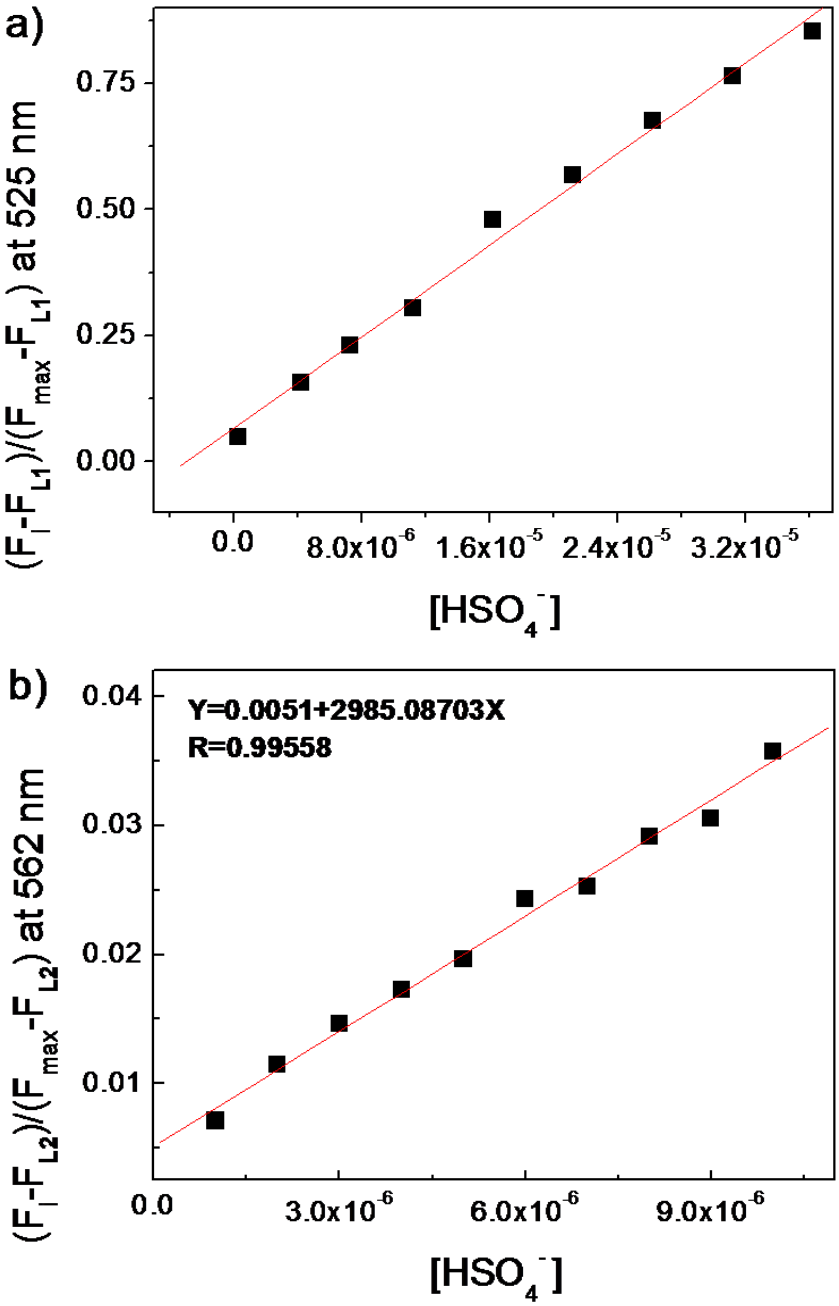

Figure S23. Detection limits of **L1** and **L2**. a) Emission at 525 nm of **L1** (6 µM) at different concentrations of HSO_4^- (0, 3.0×10^{-7}, 4.2×10^{-6}, 7.3×10^{-6}, 1.12×10^{-5}, 1.62×10^{-5}, 2.12×10^{-5}, 2.62×10^{-5}, 3.12×10^{-5}, 3.62×10^{-5}, 6.6×10^{-5} M) added, normalized between the minimum emission (0.0 M HSO_4^-) and the emission at 6.6×10^{-5} M HSO_4^-. The detection limit was determined to be 1.0×10^{-7} M. b) Emission at 562 nm of **L2** (6 µM) at different concentrations of HSO_4^- (0, 1.0×10^{-6}, 2.0×10^{-6}, 3.0×10^{-6}, 4.0×10^{-6}, 5.0×10^{-6}, 6.0×10^{-6}, 7.0×10^{-6}, 8.0×10^{-6}, 9.0×10^{-6}, 1.0×10^{-5}, 2.4×10^{-5} M) added, normalized between the minimum emission (0.0 M HSO_4^-) and the emission at 2.4×10^{-5} M HSO_4^-. The detection limit was determined to be 1.0×10^{-6} M.

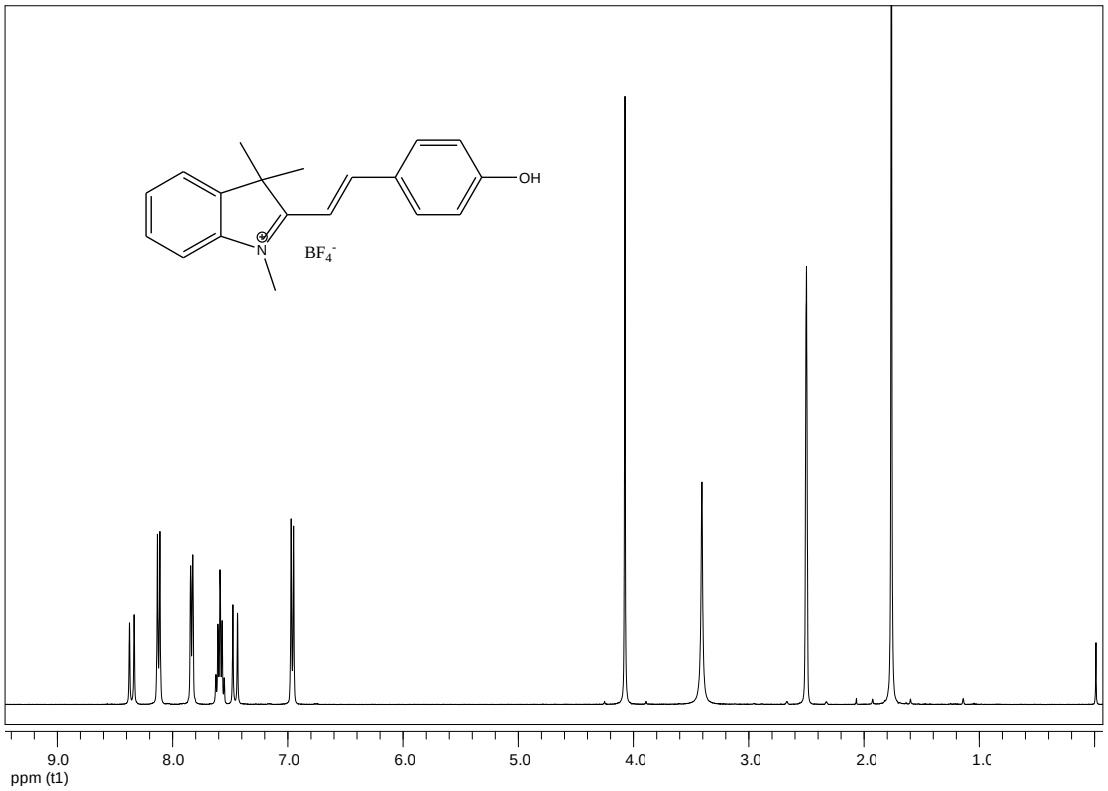

Figure S24. ^{1}H NMR of the chemosensor **L1** (400 MHz, DMSO-d_3).

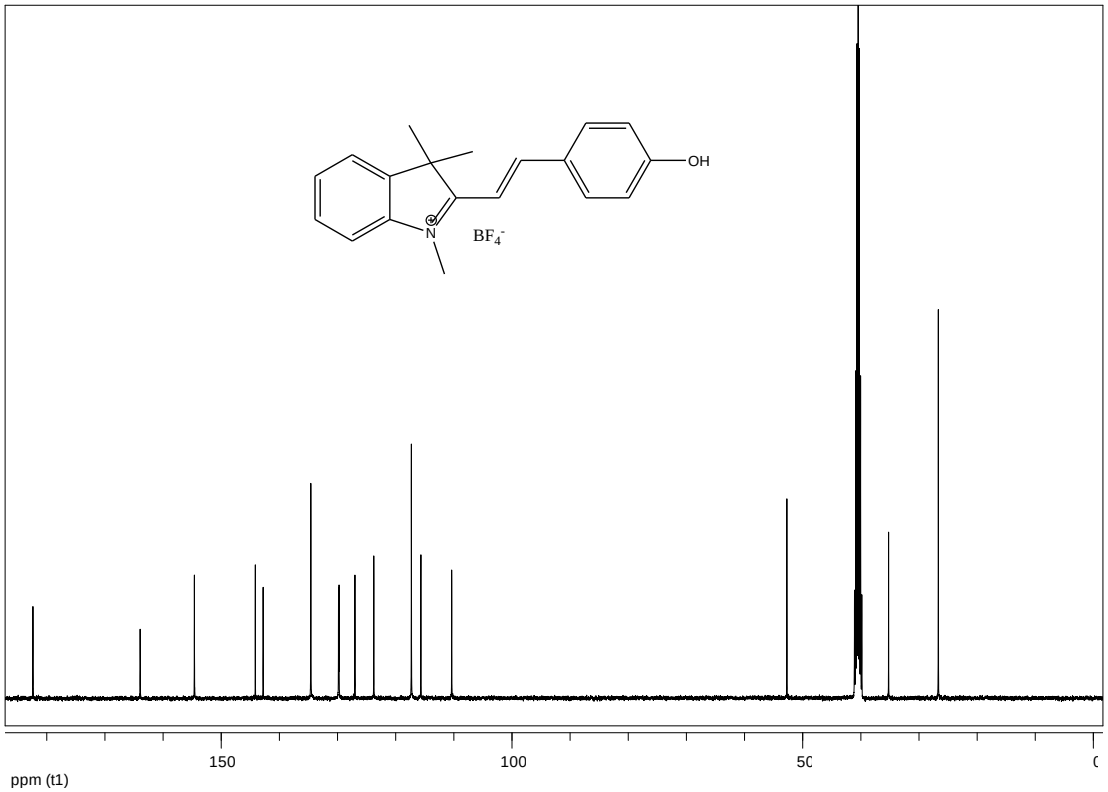

Figure S25. ^{13}C NMR of the chemosensor **L1** (100 MHz, DMSO-d_6).

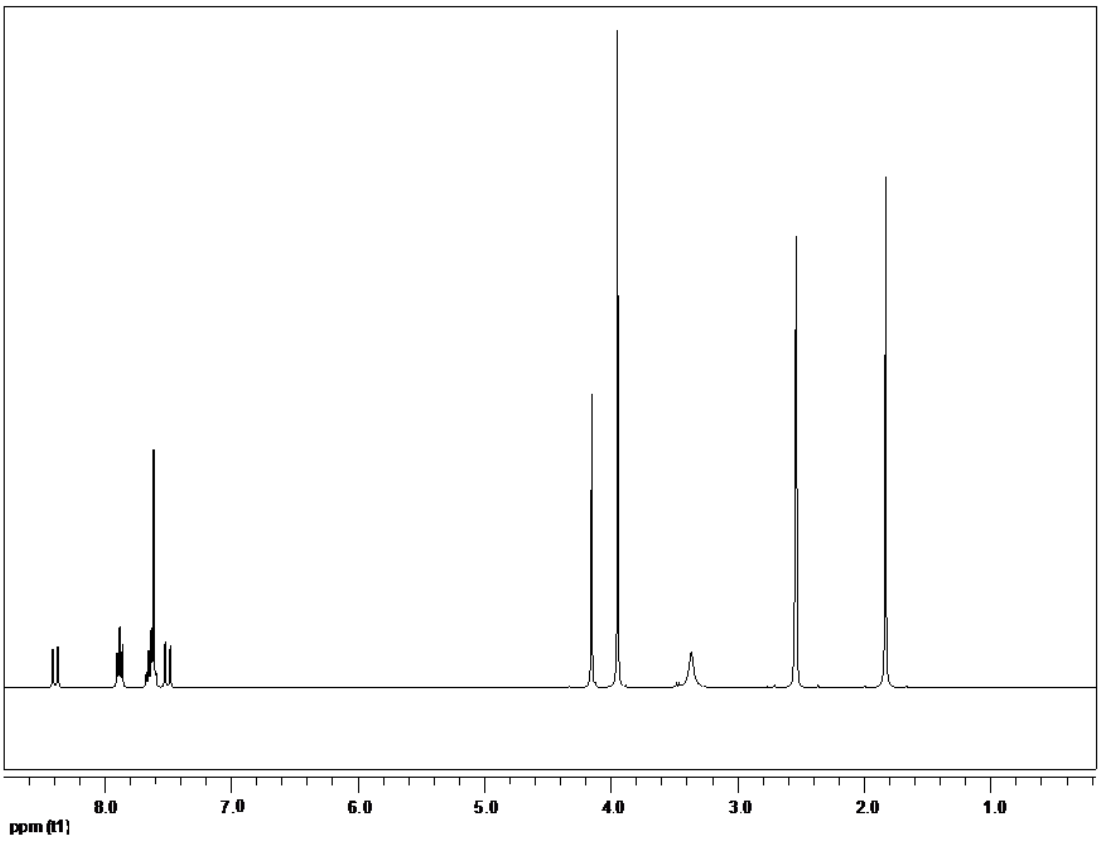

Figure S26. ^{1}H NMR of the chemosensor **L2** (400 MHz, DMSO-d_6).

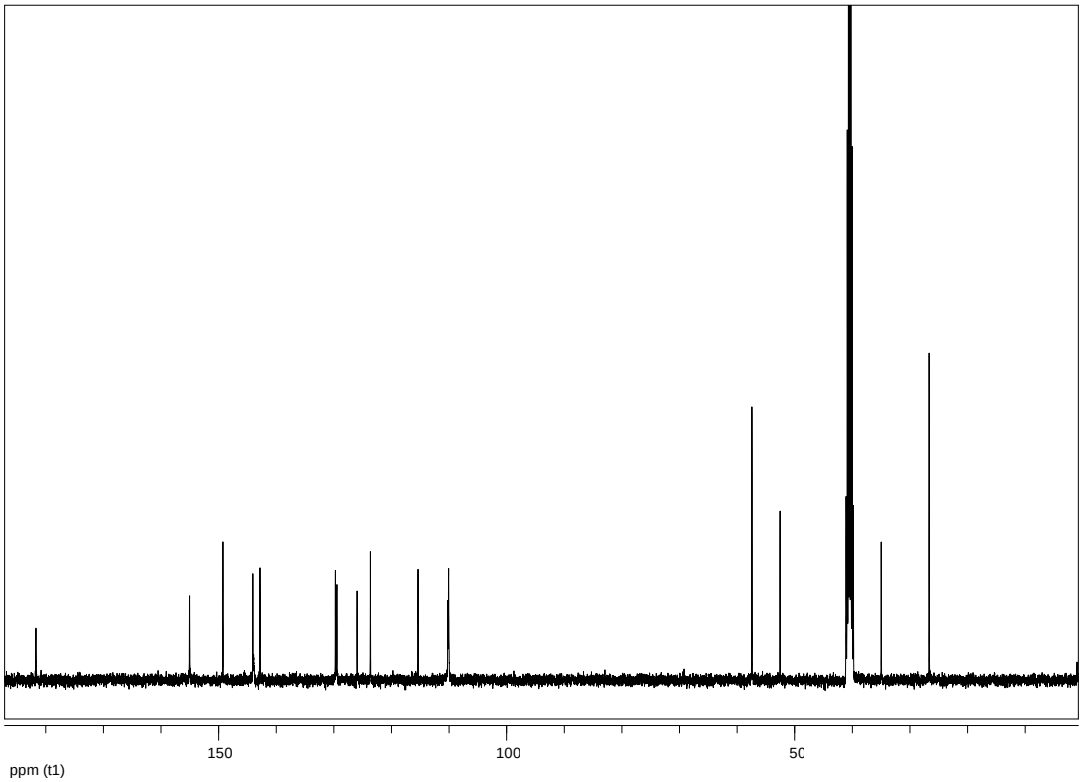

Figure S27. ^{13}C NMR of the chemosensor **L2** (100 MHz, DMSO-d_6).

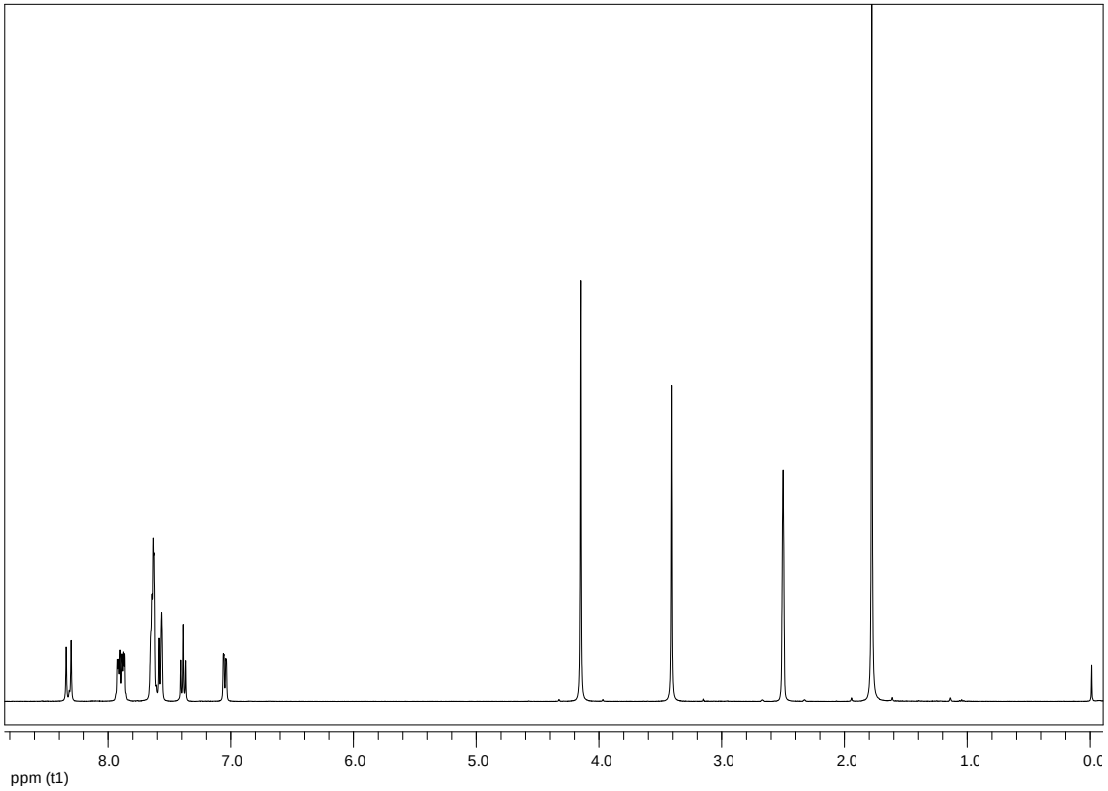

Figure S28. ^{1}H NMR of the chemosensor **L3** (400 MHz, DMSO-d_6).

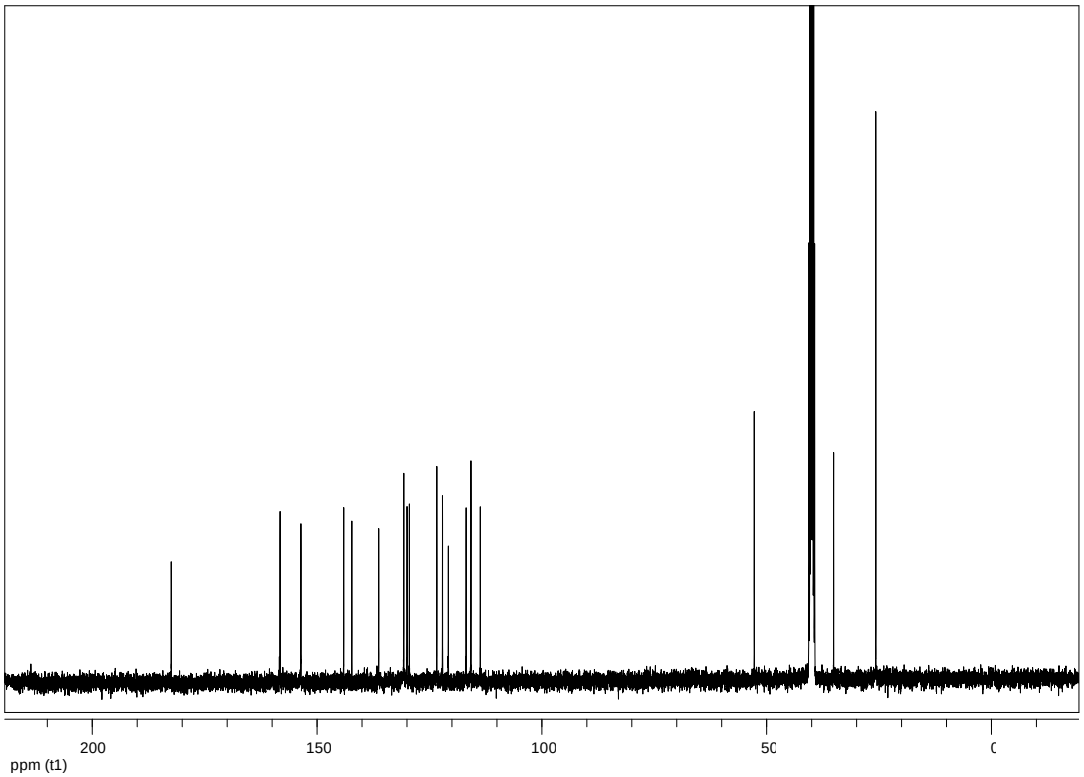

Figure S29. ^{13}C NMR of the chemosensor **L3** (100 MHz, DMSO-d_6).

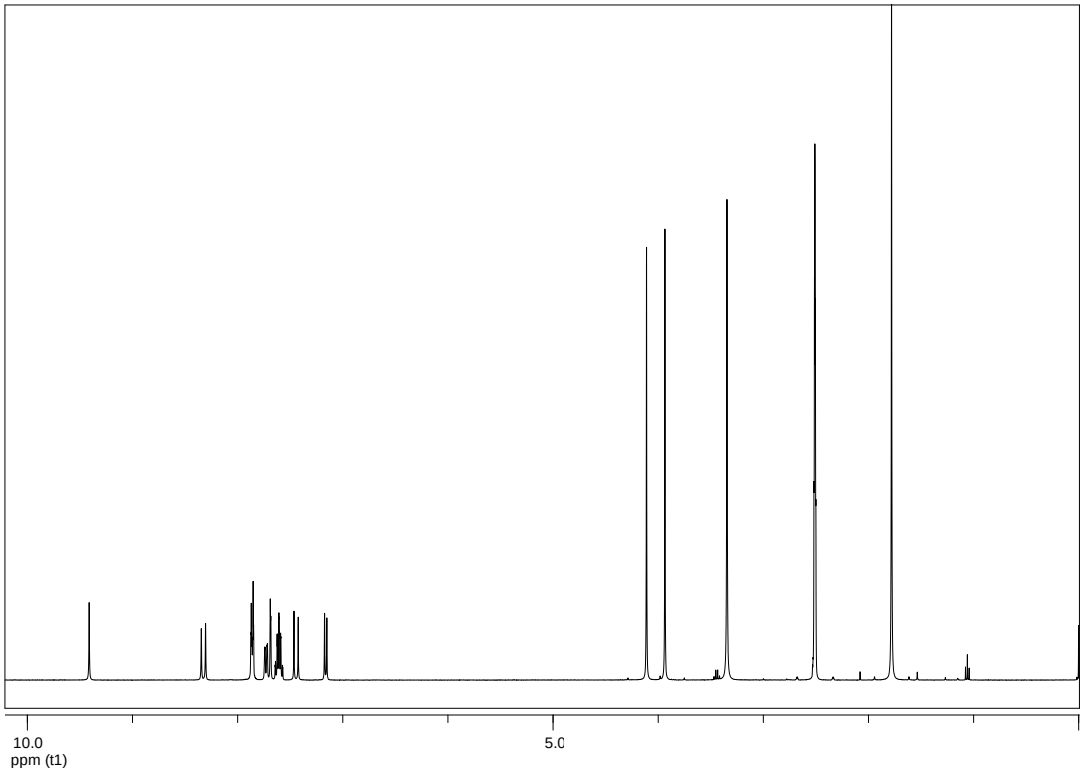

Figure S30. ^{1}H NMR of the chemosensor **L4** (400 MHz, DMSO-d_6).

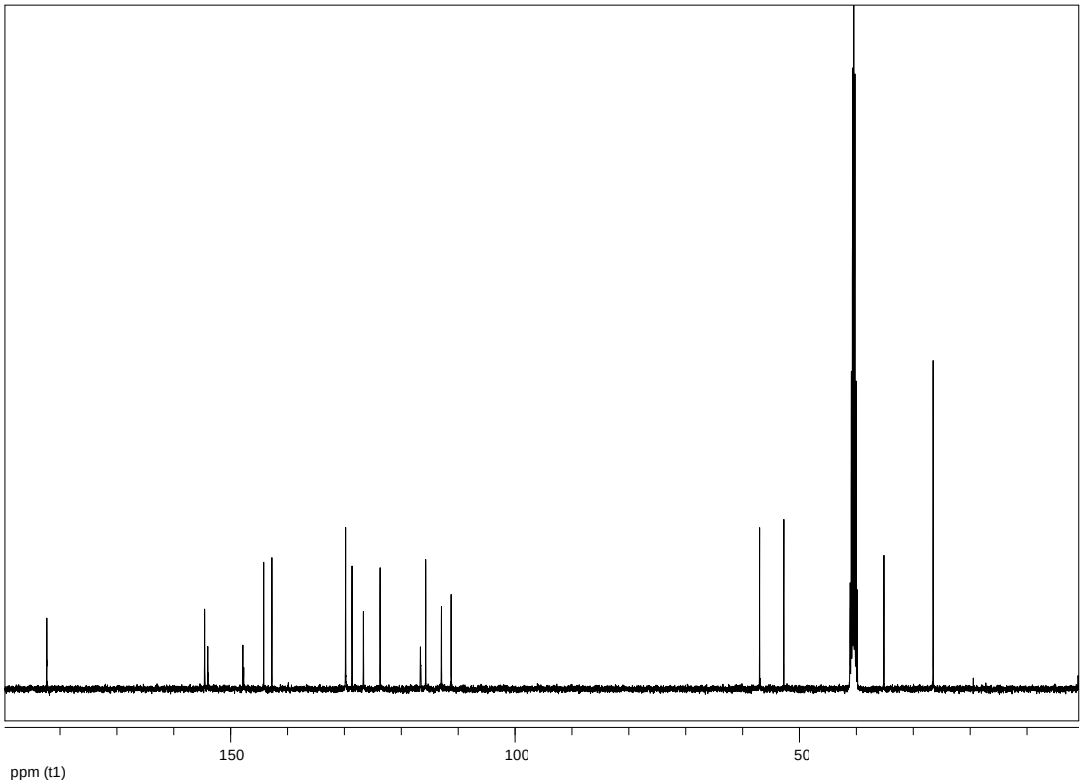

Figure S31. ^{13}C NMR of the chemosensor **L4** (100 MHz, DMSO-d_6).